

Accepted Manuscript

Title: Acetylated Cashew Gum-based Nanoparticles for Transdermal Delivery of Diclofenac Diethyl Amine

Author: Sávia Francisca Lopes Dias Silvania Siqueira
Nogueira Flaviane de França Dourado Maria Adelaide
Guimarães Nádia Aline de Oliveira Pitombeira Graciely
Gomides Gobbo Fernando Lucas Primo Regina Célia
Monteiro de Paula Judith Pessoa Andrade Feitosa Antonio
Claudio Tedesco Lívio Cesar. Cunha. Nunes José Roberto
Souza Almeida Leite Durcilene Alves da Silva



PII: S0144-8617(16)30044-3
DOI: <http://dx.doi.org/doi:10.1016/j.carbpol.2016.02.004>
Reference: CARP 10759

To appear in:

Received date: 5-10-2015
Revised date: 30-1-2016
Accepted date: 1-2-2016

Please cite this article as: Dias, S. F. L., Nogueira, S. S., Dourado, F. F., Guimarães, M. A., Pitombeira, N. A. O., Gobbo, G. G., Primo, F. L., Paula, R. C. M., Feitosa, J. P. A., Tedesco, A. C., Nunes, L. Cr. Ca., Leite, J. R. S. A., and da Silva, D. A., Acetylated Cashew Gum-based Nanoparticles for Transdermal Delivery of Diclofenac Diethyl Amine, *Carbohydrate Polymers* (2016), <http://dx.doi.org/10.1016/j.carbpol.2016.02.004>

This is a PDF file of an unedited manuscript that has been accepted for publication. As a service to our customers we are providing this early version of the manuscript. The manuscript will undergo copyediting, typesetting, and review of the resulting proof before it is published in its final form. Please note that during the production process errors may be discovered which could affect the content, and all legal disclaimers that apply to the journal pertain.

1 Acetylated Cashew Gum-based Nanoparticles for 2 Transdermal Delivery of Diclofenac Diethyl Amine

3 Sávia Francisca Lopes Dias^a, Sylvania Siqueira Nogueira.^a Flaviane de França
4 Dourado^a, Maria Adelaide Guimarães^a, Nádia Aline de Oliveira Pitombeira^c,
5 Graciely Gomides Gobbo^d Fernando Lucas Primo^d, Regina Célia Monteiro de
6 Paula^c, Judith Pessoa Andrade Feitosa^c, Antonio Claudio Tedesco^d, Lívio Cesar.
7 Cunha. Nunes^b José Roberto Souza Almeida Leite^a, Durcilene Alves da Silva^{a*}

8

9a. UFPI, Research Center in Biodiversity and Biotechnology - Biotech Campus Parnaíba, Federal
10 University of Piauí, Av São Sebastian 2819, 64202-020, Parnaíba, Piauí, Brazil

11b. UFPI, Center for Pharmaceutical Technology, Federal University of Piauí, Teresina, Brazil.

12c. UFC, Polymer Laboratory, Federal University of Ceará, Fortaleza, Brazil.

13d. USP, Department of Chemistry, Laboratory of Photobiology and Photomedicine, Center
14 Nanotechnology and Tissue Engineering, University of São Paulo, Ribeirão Preto, Brazil.

15

16

17 ABSTRACT

18 Nanoprecipitation and dialysis methods were employed to obtain nanoparticles (NPs) of
19 acetylated cashew gum (ACG). NPs synthesized by dialysis showed greater average size
20 compared to those synthesized by nanoprecipitation, but they presented improved
21 stability and yield. NPs were loaded with diclofenac diethylamine and the efficiency of
22 the drug incorporation was over 60 % for both methods, for an ACG:NP a weight ratio
23 of 10:1. The cytotoxicity assay demonstrated that the NPs had no significant effect on
24 the cell viability, verifying their biocompatibility. The release profile for the diclofenac
25 diethylamine associated with the ACG-NPs showed a more controlled release compared
26 to the free drug and a Fickian diffusion mechanism was observed. Transdermal
27 permeation reached 90 % penetration of the drug.

28 Keywords: nanoparticles; acetylated cashew gum; Diclofenac diethyl amine;
29 cytotoxicity; transdermal delivery

30

31

32 Chemical compounds

33 acetone (CID: 180); acetonitrile (CID: 6342); acetic anhydride (CID: 7918); diclofenac
34 diethylamine (CID:115087); dimethyl sulfoxide (CID:679); ethanol (CID:702);
35 formamide (CID: 713); phosphoric acid (CID:1004); pyridine (CID: 1049); sodium
36 hydroxide (CID: 14798).

37 *Mailing address of corresponding author: Center for Biodiversity Research and
38 Biotechnology (BIOTEC), Federal University of Piauí, Campus Minister Reis Veloso,
39 Parnaíba, Piauí. Avenida São Sebastião, CEP 64202020

40 Phone: +55 86 33235433

41 E-mail: durcileneas@yahoo.com.br

42

43

44 1. Introduction

45

46 In the area of pharmaceutical technology differentiated systems have been
47 developed for targeted drug delivery. In this regard, polymeric materials have received
48 more attention than other classes of materials in the development of drug delivery
49 systems (Kim et al., 2009). Certain properties of polysaccharides, such as
50 biodegradability and biocompatibility, mean that many researchers have selected these
51 polymers for the preparation of biomaterials (Liu et al., 2008).

52 Cashew gum (CG) is a polysaccharide extracted from an affordable and easily
53 available source, that is, the species *Anacardium occidentale*, which is widely
54 distributed in northeastern Brazil. Purified cashew gum contains galactose (72-73%),
55 glucose (11-14%), arabinose (4.6 to 5%), rhamnose (3.2-4%) and glucuronic acid (4.7
56 to 6.3%) in its structure (Paula and Rodrigues, 1995; Paula, de Paula, Heatley, & Budd,
57 1998).

58 In the biomedical field some potential applications of cashew gum are already
59 known, for instance, it acts as an anti-inflammatory agent in the healing of mice
60 (Shirato et al., 2006), shows significant antibacterial activity (Torquato, 2004; Campos,

61 2012), is an excellent film forming material, with potential application in
62 nanobiomedical devices (Araújo et al., 2012), and it has demonstrated an *in vivo* anti-
63 tumor effect (Florêncio, Melo Mota, Melo-Junior & Araújo, 2007). In the
64 pharmaceutical area it has been reported that cashew gum can act as a gelling agent in
65 the topical formulation of aceclofenac (Kumar, Patil, Patil, & Paschapur, 2009) and as a
66 binder for paracetamol tablets (Gowthamarajan et al., 2011). Also, it is used to
67 produce curcumin tablets with buccal adhesive ability and thus circumvent hepatic
68 metabolism and improve the bioavailability of the active principle (Gowthamarajan et
69 al., 2012).

70 However, there are some difficulties associated with the use of gums, such as a
71 drop in viscosity during storage and the possibility of microbial contamination.
72 Chemical modification not only minimizes these disadvantages but also allows more
73 specific drug delivery (Rana et al., 2011) and it can improve the efficiency of the
74 incorporation of the drug into the matrix (Zhang et al., 2009).

75 Cashew gum nanoparticles grafted with acrylic acid were obtained by radical
76 polymerization using Ce (IV) ions as the initiator and methylene-bis-acrylamide as the
77 crosslinker. Nanoparticles which are pH-sensitive were obtained with sizes in the range
78 of 71-603 nm, depending on the gum/acrylic acid ratio (Silva et al. 2009). Nanoparticles
79 based on carboxymethylated cashew gum (CMCG) and chitosan were synthesized with
80 diameters ranging from 150 to 400 nm. Smaller particle sizes were obtained for CMCG
81 samples with a lower degree of substitution (DS) (Silva et al., 2010).

82 In a previous study, acetylated cashew gum (ACG) with a DS of 2.8 was
83 synthesized and self-assembled nanoparticles were obtained through the dialysis of an
84 organic solution (DMSO) against a non-solvent (water). The mean diameter of the self-
85 assembled nanoparticles obtained was 179 nm and the critical aggregation concentration

86 (CAC) in water was 2.1×10^{-3} g/L. Indomethacin (IND) was used as a hydrophobic
87 model drug and was incorporated into the hydrophobized polysaccharide nanoparticles.
88 A controlled drug release was observed for up to 72 h (Pitombeira et al., 2015).

89 Nanoparticles (NPs) as polymeric carriers of drugs have been the subject of
90 several reviews in the literature (Liu et al., 2008; Langer & Tirrell, 2004; Uhrich, et al.,
91 1999; Peppas, 1995; Soppimath et al., 2001; Singh & Lillard, 2009; Oh, Lee & Park,
92 2009; Kumari Yadav & Yadav, 2010). In this context, anti-inflammatory drugs
93 (NSAIDs) are frequently the drug investigated, in an attempt to overcome some
94 difficulties related to their pharmacokinetics and pharmacodynamics, as well as several
95 adverse effects resulting from their oral and parenteral administration, such as gastric
96 irritation and ulceration (Beck et al., 1990; Galer, et al. 2000; Jones & Rubin, 2008).
97 Nanoencapsulation in polymeric systems protects the drug and contributes to a
98 controlled release, thus increasing the therapeutic benefit with minimal side effects
99 (Soppimath, et al., 2001). The transdermal route also reduces these side effects,
100 increases patient compliance, avoids hepatic metabolism, and maintains the plasma drug
101 concentration for a longer period (Shakeel et al., 2007; Prow et al., 2011).

102 In this study, different methods for the preparation of acetylated cashew gum
103 (ACG) nanoparticles were investigated and studies on the incorporation, release and
104 cutaneous permeation of diclofenac diethylamine were carried out, as a proof-of-
105 concept for a transdermal drug delivery device.

106

107 **2. Materials and Methods**

108 **2.1 Materials**

109 Diclofenac diethylamine (DDA) was purchased from Henrifarma, Teresina, lot
110 10100025. The cashew gum (CG) was isolated from a tree of the species *Anacardium*

111 *occidentale* ($M_w = 1.8 \times 10^5$ g/mol) using an adapted method previously described by
112 Paula, Heatley and Budd (1998). The exudate was dissolved in distilled water at room
113 temperature to give a 10% (w/v) solution. The pH was adjusted to approximately 7.0 by
114 addition of diluted aqueous sodium hydroxide. The clear solution was successively
115 filtered through sintered glass and the polysaccharide precipitated with ethanol at ratio
116 of 1:3 (gum solution: ethanol). The precipitate (isolated gum) was dried in a forced air
117 oven at 60°C/8 h and weighed.

118 All other reagents were of analytical grade (Formamide, pyridine, acetic
119 anhydride, dimethyl sulfoxide, sodium hydroxide, ethanol, acetone were purchased from
120 Vetec and acetonitrile and phosphoric acid were purchased from Sigma-Aldrich)

121

122 **2.2 Acetylation of cashew gum**

123 The acetylated cashew gum (ACG) was synthesized by Motozato's method
124 (1986) as reported in Pitombeira et al. (2015) with a degree of substitution of 2.8.
125 Cashew gum (1 g) was suspended in 20 ml of formamide under vigorous stirring.
126 Pyridine (3 g) and acetic anhydride (7 g) were added and the mixture was stirred for 24h
127 at 50°C. The ACG was obtained by precipitation with 400 mL of water. The solid was
128 filtered, washed with water and dried in hot air.

129 The polysaccharide obtained was characterized by infrared spectroscopy and
130 nuclear magnetic resonance spectroscopy. FT-IR spectra were recorded with KBr
131 pellets on an FT-IR Shimadzu 8300 spectrophotometer in the range of 4,000 to 400
132 cm^{-1} , with a resolution of 2 cm^{-1} and 15 scans. ^1H NMR spectra of 3% w/v solutions in
133 DMSO- d_6 were recorded at 353 K on a Fourier transform Bruker Avance DRX 500
134 spectrometer with an inverse multinuclear gradient probe-head equipped with z-shielded

135 gradient coils and a Silicon Graphics workstation. Sodium 2,2-dimethylsilapentane-5-
136 sulphonate (DSS) was used as the internal standard (0.00 ppm for ^1H).

137 **2.3 Preparation of ACG nanoparticles**

138 The synthesis of the nanoparticles was performed using two different methods:
139 nanoprecipitation and dialysis (Raoa and Geckeler, 2011). Identical procedures were
140 conducted for the synthesis of NPs containing the drug. In both methods the ACG was
141 dissolved in 20 mL (0.1% w/w) of acetone for 15 min under magnetic stirring.
142 Diclofenac diethylamine (DDA) is a hydrophobic drug and it was incorporated into the
143 ACG nanoparticles at the time of their synthesis. The drug-loaded nanoparticles
144 obtained are referred to herein as ACG-DDA-NPs. For both methods investigated three
145 polymer/drug proportions (by weight) were studied (10:1, 10:2 and 10:5).

146

147 **2.3.1 Nanoprecipitation**

148 A solution of ACG in acetone (0.1%w/w) was dispersed in 20 mL of deionized
149 water in a homogenizer (Ultra Turrax T25 Basic Heidolpha) at 19,000 rpm. Removal of
150 the solvent by evaporation was carried out in a Heidolph RZR205 rotoevaporator system
151 at 40°C. The material was then filtered with a 0.45 μm syringe filter and the solution
152 centrifuged at 20,000 rpm for 2 h for purification of the polymer.

153

154 **2.3.2 Dialysis**

155 A solution of ACG in acetone (0.1%w/w) was dialyzed against deionized water
156 using a cellulose acetate membrane (molecular weight 12,000) for 24 h. The
157 conductivity was used to monitor the water exchange. The resulting solution was then
158 lyophilized.

159

160 **2.4 Amount of drug encapsulated and the encapsulation efficiency (%EE)**

161 The amount of DDA in the nanoparticles was determined by UV-Vis
 162 spectroscopy at 276 nm. The analysis was performed on a Shimadzu UV-1800
 163 equipment, coupled to a standard PC and operated via UV probe software 2:33. Quartz
 164 cells were used and readings were taken between 190 and 400 nm. The amount of
 165 encapsulated diclofenac was calculated using a calibration curve to determine the
 166 relationship between the absorbance and the concentration ($R^2= 0.9998$ and $Y = 0.290 +$
 167 $28.58X$). The drug load (%) and drug efficiency (%EE) were calculated as

168 ***Drug Load (%DL)***

$$169 \frac{\text{Mass of drug in nanoparticle} \times 100}{\text{Mass of drug} + \text{mass of nanoparticle}} \quad (1)$$

170 ***Encapsulation efficiency (%EE)***

$$171 \frac{\text{Mass of loaded DDA} \times 100}{\text{Mass of added DDA}} \quad (2)$$

172

173 **2.5 Dynamic light scattering (DLS) and zeta potential**

174 The particle size and zeta potential were determined on a Malvern Zetasizer
 175 Nano ZS Model 3600 analyzer. The hydrodynamic diameter was measured by dynamic
 176 light scattering (DLS), using a 633 nm laser at a fixed scattering angle of 173°. The
 177 particle size was obtained considering the particle as spherical-like. Each sample was
 178 measured in triplicate and is reported as the mean \pm SD (n=3).

179 **2.6 Scanning electron Microscopy (SEM)**

180 The scanning electron microscopy was recorded using a Jeol-6360LV field
 181 emission. To prepare the SEM sample, a drop of nanoparticles was deposited on carbon
 182 stickers on aluminum stubs, dried and coated with gold.

183

184 **2.7 *In vitro* DDA release assay**

185 The release profiles for the free DDA and the drug-loaded nanoparticles (ACG-
 186 DDA-NPs) were obtained using a dialysis system. A sample (6 mg) of the ACG-DDA
 187 NPs was introduced into cellulose acetate membrane with molecular exclusion pores of
 188 12,000 Da and dialyzed against 50 mL of phosphate buffer solution (PBS), pH 7.4 at
 189 37°C for 24 h.

190 Aliquots of 1.5 ml were withdrawn every 30 min and the drug concentration
 191 was quantified by UV-vis spectroscopy. The buffer was replenished to keep the volume
 192 constant. The measurements of the absorbance at a wavelength at 276 nm were
 193 converted into the percentage of drug released according to a previously established
 194 calibration curve for which the linearity was confirmed ($R^2 = 0.999$). The experiment
 195 was performed in triplicate and the drug concentrations were corrected considering the
 196 dilution factor. To understand the mechanism of drug release from the nanoparticles, the
 197 data were treated according to the Korsmeyer-Peppas model (Peppas, 1985) described
 198 by Equation 3.

$$199 \frac{Q_t}{Q_0} = kt^n \quad (3)$$

200

201 where Q_t is the amount of drug released at time t , Q_0 is the amount of drug in the
 202 solution, k is a kinetic constant and n is the release exponent, which, according to the
 203 resulting numerical values, characterizes the mechanism of drug release. The

204 linearization of Equation 3 through the construction of $\ln Q_t/ Q_0$ as a function of $\ln t$,
205 provides the release exponent (n) and constant release (k).

206 **2.8 *In vitro* permeation assay**

207 Vertical Franz-type diffusion cells ($n=5$) with a diffusional area of 1.77 cm^2
208 were used for the permeation study. The skin used in the tests was taken from the dorsal
209 surface of pig ears and kept refrigerated at -80°C until use. The skin was carefully
210 placed between the donor and receiver compartment of each cell, the latter of which was
211 filled with 7 mL of phosphate buffer solution (pH 7.4), so that the dermis was in direct
212 contact with this medium. The temperature was maintained at 37°C with stirring at 400
213 rpm.

214 Permeation assay was prepared as follows: A volume of 200 μL of the ACG-
215 DDA-NPs formulation in phosphate buffer (pH 7.4) at 0.5 mg/mL was placed in the
216 donor compartment. Aliquots (1.5 mL) were withdrawn at predetermined periods and
217 analyzed by high performance liquid chromatography (Sintov, et al (2006). For this
218 purpose we used a MERCK HITTACHI L-7000 chromatograph with a UV detector (L-
219 7400 LACHROM) at 276 nm and a C18 reverse phase column (250 x 4.6 mm) with a
220 particle size of $5\mu\text{m}$. The mobile phase consisted of a mixture of acetonitrile: water with
221 0.1% phosphoric acid (98:2 v/v) with a final pH of 3.5. The chromatography was
222 performed at room temperature with a flow rate of 0.6 ml min^{-1} and automatic injection.

223 The same amount of buffer was added to keep the volume constant and the free
224 DDA was also measured in order to compare the permeation profile. The data were
225 expressed as the amount of drug permeated by the surface area of the skin ($\mu\text{g}/\text{cm}^2$).

226

227 **2.9 Cytotoxicity test**

228 The cell line used in this study was an oral squamous cell carcinoma (OSCC)
229 obtained from the American Type Culture Collection (ATCC, Manassas, VA). Cells (5
230 $\times 10^4$ cells/mL) were grown in 75 cm² flasks on 96-well plates and maintained in
231 Dulbecco's modified Eagle medium (DMEM) supplemented with 10% fetal bovine
232 serum (FBS), 1% L-glutamine, 1 % penicillin-streptomycin and 0.25% amphotericin B.
233 The cells were treated with ACG-NPs, ACG-DDA-NPs and DDA at different
234 concentrations for 3 h in an incubator (5% CO₂ at 37 °C, humidified atmosphere of
235 33%). Control cells were incubated with culture medium alone. After 24 h, DMEM
236 without phenol red and 3-(4,5-dimethylthiazol-2yl)-2,5-diphenyl tetrazolium bromide
237 (MTT) were added to each well and the plates were incubated for 4 h at 37°C (5% CO₂,
238 humidified atmosphere of 33%).The formazan crystals formed were dissolved in 2-
239 propanol and evaluated at 560 and 690 nm using a Safire² multiplate reader.

240 **2.10 Statistical analysis**

241 Statistical analyses were performed applying one-way ANOVA and the Tukey
242 test using Prisma software. All data reported in the tables and figures are expressed as
243 the mean \pm SEM of three independent experiments. Statistical significance for this study
244 was considered as $p < 0.05$.

245

246 **3.0 Results and Discussion**

247 The acetylated polysaccharides were characterized by infrared spectroscopy and
248 according to the spectra in the infrared region, the intensity of vibrations at 3400 cm⁻¹
249 present in cashew gum (CG) decrease as the acetyl groups are inserted (Fig. 1 a). The
250 absorption bands at 1375 cm⁻¹ and 1752 cm⁻¹ are typical of ester groups demonstrating
251 the acetylation of the polymer (Fig. 1 b). The acetylated polysaccharide shows yield of

252 65% and the same degree of substitution (2.8) observed previously by Pitombeira et al.
253 (2015), and calculated using the $^1\text{H-NMR}$ spectra (figure not shown).

254 Several polysaccharides like dextran, chitosan and pululan have been chemically
255 modified to improve their physico-chemical, mechanical or chemical-biological
256 properties, expanding the possibilities of using it in new materials (Lemarchand, Gref,
257 Couvreur, 2004). In the last decade there has been increased interest in developing these
258 modified polysaccharides for the synthesis of biodegradable nanoparticles. Due to the
259 fact that these structures showed many advantages for biomedical applications such as
260 drug protection and the ability to control its release (Rodrigues et al., 2003; Leonard et
261 al., 2003; Chourasia and Jain, 2004; Chourasia et al., 2006; Singh and Kim, 2007;
262 Zhang et al., 2009).

263 **3.1 Characterization of ACG nanoparticles**

264 Certain variables determine the success of nanoparticle synthesis and affect the
265 physico-chemical properties of the nanoparticles obtained. These include the conditions
266 under which the organic phase is added to the aqueous phase and the concentration of
267 the material involved (Rao and Geckeler 2011).

268 The NPs prepared by dialysis using acetone as the solvent had larger particles
269 (302 nm) than those obtained using DMSO as solvent (179 nm). NPs synthesized by
270 nanoprecipitation showed smaller average size (79.37 nm) compared to those
271 synthesized by dialysis (302 nm), however a more negative zeta potential and smaller
272 polydispersity index (PDI) values were observed for NPs synthesized by dialysis (Table
273 1). According to Mohanraj & Chen (2006), values lower than 0.2 for the polydispersity
274 and above 30 mV for the zeta potential (in module) indicate good colloidal stability in
275 solution. Thus, the particles prepared by dialysis presented better colloidal stability than
276 those prepared by nanoprecipitation.

277 Under similar conditions, for NPs of dextran hydrophobically modified and
278 with ibuprofen incorporated, Horning, Bunje & Heinze (2009) reported particle sizes of
279 309 nm obtained through dialysis and 77 nm for synthesis via nanoprecipitation. These
280 results are quite similar to those observed in the study reported herein. Figure 2 shows
281 the particle size distribution for nanoparticles with and without the drug. In Figure 3 it is
282 possible to observe the SEM image of ACG NPs. The image shows spherical particles
283 and the sizes determined by SEM were in the ranges of 150-280 nm and 300-450 for
284 DDA ACG NP and ACG nanoparticles, respectively.

285 For both methods investigated, the addition of the drug decreases the
286 polydispersity index. No tendency in relation to the particle size was observed on
287 changing the nanoparticle:DDA ratio (Table 2). On applying the nanoprecipitation
288 method, a significant increase in particle size ($p < 0.001$) was observed for all
289 nanoparticle:DDA ratios investigated, whereas in the case of dialysis a significant
290 reduction in the particle size was observed for a nanoparticle:DDA ratio of 10:1, and for
291 other ratios no statistically significant variation was observed (Table 2).

292 Increasing the nanoparticle:drug ratio to 10:5 promoted a decrease in the
293 encapsulation efficiency (%EE). For the lowest drug concentration (10:1) the amount
294 incorporated was higher than 60% for both methods (Table 2). With respect to the drug
295 loading (DL), the highest value was obtained for a nanoparticle:drug ratio of 10:2 for
296 both methods, although this ratio did not provide the highest encapsulation efficiency in
297 the case of the dialysis method. Using dialysis and nanoprecipitation, Horning, Bunjes
298 & Heinze (2009) obtained the same %EE (46.5%) for both methods. However, in other
299 studies, lower values for the incorporation of the drug into NPs synthesized through
300 dialysis were noted, for instance, Shi & Shoichet (2008) observed a DL of <1% and
301 Ericco et al. (2009) reported a DL of 2.2%.

302 Therefore, based on the results obtained for particle size, zeta potential, yield
303 and %EE, the nanoparticles produced by the dialysis method with a ACG-NPs:drug
304 ratio of 10:1 were chosen for the *in vitro* release and permeation studies as well as for
305 cell viability assays.

306

307 **3.2 Cytotoxicity**

308 Figure 4 shows the *in vitro* cytotoxicity of the ACG-NPs and ACG-DDA-NPs
309 using the previously grown OSCC cell line as described above. Nanoparticles in
310 different concentrations were added to the cell suspension and left for 24 h at 37°C. The
311 cell viability was subsequently measured using the MTT assay (Fig. 4). The
312 nanoparticles (with or without the DDA) did not show any basal toxicity up to a
313 concentration of 150 µg/mL. Recently, similar results were obtained
314 for polymeric modified NPs, with and without doxorubicin, under physiological
315 conditions (Thambi et al., 2014).

316 Another study using 10 µg/ml of methotrexate indicated that there was no
317 significant difference between the effects of the free drug and the drug incorporated in
318 chitosan nanoparticles on tumor cells of the MCF-7 lineage and non-tumor cells
319 (Nogueira et al., 2013).

320 However, it's possible to see that a slight reduction in cell viability in the
321 presence of acetylated cashew gum, even if this difference is not significant, this may be
322 due to cell line type, the dosage or the chemical composition of the gum. Sarika et al.
323 (2015) developed Arabic gum-curcumin conjugate micelles (GA-cur), and evaluated
324 cytotoxicity by MTT assay using on MCF-7 and HepG2 cells. At concentration of 3.125
325 g/mL show non_cytotoxic to MCF-7, but cytotoxic was observed for HepG2 cells.
326 Rigopoulou et al. (2012) reported that the presence of galactose moiety in the structure

327 of gum arabic can selectively identify asialoglyco protein receptor (ASGPR) on the
328 surface of hepatocytes.

329 David et al. (2015), reported the cell viability studies when MiaPaCa2 cells were
330 incubated with quercetin-loaded chitosan nanoparticles, blank chitosan nanoparticles
331 and free quercetin. Blank chitosan nanoparticles did not exhibit significant changes in
332 the cell viability. In addition, no significant difference in cell viability was observed for
333 free quercetin between 10 and 100 μM . In comparison, quercetin-loaded chitosan
334 nanoparticles exhibited significant reduction in the cell viability in a dose-dependent
335 manner.

336 **3.3 Release kinetics and *in vitro* permeation**

337 The drug release was analyzed by diffusion through a dialysis membrane in
338 phosphate buffer solution. Figure 5A, 5B shows the release profile for the anti-
339 inflammatory drug (DDA) encapsulated in ACG nanoparticles and free DDA. It can be
340 observed that the DDA was released from the ACG-NPs in a controlled manner, with a
341 burst effect within the first 5 h followed by a more uniform release up to 24 h, after
342 which a release of around 60% was achieved. Similar results were observed for sulfated
343 chitosan NPs loaded with curcumin, with an average NP size of 220 nm and a
344 maximum release rate of 70% (Anitha et al., 2011). Another study showed similar
345 results for acetylated pullulan NPs loaded with epirubicin, with NPs of > 200 nm and
346 controlled release rates of up to 60% (Zhang et al., 2009). Although Martins et al.
347 (2012) reported a release of less than 20% for heparin from chitosan microparticles they
348 obtained the release profile in two steps. The biphasic release behavior is consistent to
349 the results obtained by Chin et al., (2014) and Ayadi et al., (2016). These authors
350 verified that the initial fast release was due to the presence of drug adsorbed onto the
351 nanoparticle surface or held close to it.

352 Liu and He (2015) reported the release of aspirin and probucol drugs from
353 modified chitosan nanoparticles, both aspirin and probucol were released rapidly in the
354 first 24h, and the release rate decreased significantly thereafter. The cumulative release
355 amount of probucol was much higher than that of aspirin in the data range, which can be
356 due the different interactions of aspirin and probucol with the modified chitosan
357 nanoparticles matrix.

358 In order to investigate the mechanism through which the drug was released
359 from the nanoparticles the Korsmeyer-Peppas equation was applied as shown in Fig. 6
360 A release exponent (n) value of 0.27 was obtained, indicating Fickian diffusion. The
361 release of indomethacin from acetylated cashew gum also showed a Fickian diffusion
362 mechanism (Pitombeira et al., 2015).

363 Similar release profiles have also been observed by using other diclofenac
364 release systems. For instance, Liu et al. (2010) reported a slow release rate of diclofenac
365 when encapsulated in solid lipid nanoparticles. Silva et al. (2014) confirms the capacity
366 of bacterial cellulose (BC) membrane loaded with diclofenac to provide a sustained
367 release, which can be successfully combined with a good biocompatibility_ and
368 absorption properties.

369 The transdermal permeation profile for the drug incorporated into ACG-DDA-
370 NPs compared to free DDA can be observed in Fig. 7. Both the free drug and the drug
371 associated with the nanoparticles reached a permeation of approximately $1.5 \mu\text{g}/\text{cm}^2$ in
372 six hours of testing, which is equivalent to an average of 90% permeated DDA.
373 However, the nanostructured system demonstrates a more controlled permeation profile
374 which is maintained over time.

375 Sintov & Botner (2006) also confirmed the controlled and effective transdermal
376 penetration of sodium diclofenac from a microemulsion *in vitro*. However, in contrast to

377 the results obtained in this study, they observed significantly higher permeation values
378 for the microemulsion compared with the application of the drug in aqueous solution.
379 However, it should be noted that sodium diclofenac, unlike diethylamine, does not show
380 effective transdermal permeation due to its physico-chemical properties.

381 Minghetti et al. (2007) investigated the effects of three skin penetration
382 enhancers, on four diclofenac salts, the maximal amount of diethylamine diclofenac
383 permeated from the aqueous vehicles were 2–4 fold greater than the amounts permeated
384 when compared with all other salts and vehicles. The possibility of diclofenac
385 micellization in aqueous systems was considered as one of the contributors to the
386 favorable skin penetration.

387 Sodium diclofenac was also incorporated into different nanoemulsions and
388 once again it was possible to verify that nanoemulsions are effective accelerators for the
389 permeability of the drug through the skin. The nanosize of the formulations was
390 suggested by the authors as a permeation enhancer (Piao et al., 2007). Likewise, PLGA
391 and chitosan were used to prepare a bilayered system of nanoparticles for the
392 simultaneous topical delivery of two anti-inflammatory drugs and it was found that the
393 skin permeation of the nanostructures was much higher when compared to the
394 commercial topical gel (Shah et al., 2012).

395

396 **4. Conclusions**

397

398 In this study, acetylated cashew gum nanoparticles were successfully prepared
399 via two different methods. The nanostructures were incorporated in DDA and showed
400 great potential as carriers for controlled drug release systems as well as transdermal
401 permeation promoters *in vitro*. The high rates of cell viability indicate that the NPs offer

402 good biocompatibility, with and without the drug incorporated. This means that ACG
403 may be useful for the delivery of anti-inflammatory drugs, however comparative studies
404 with a commercial formulation and *in vivo* assays have yet to be performed.

405

406 **Acknowledgements**

407 This research was conducted in partnership with the Laboratory of Polymers,
408 Federal University of Ceará where the polymer modification was carried out and the
409 Laboratory of Nanomedicine, Nanotechnology and Tissue Engineering, University of
410 São Paulo (USP, Ribeirão Preto), responsible for *in vitro* permeation and cytotoxicity
411 studies. The authors are grateful to Vegeflora of the Centroflora Group for the analysis
412 of the HPLC efficiency. The authors also acknowledge CNPq and CAPES for a
413 scholarship and financial aid.

414

415 **5. References**

416

417 Anitha A., Deepagan V.G., Rani V.V. D., Menon D., Nair S.V., Jayakumar R., (2011)
418 Preparation, characterization, *in vitro* drug release and biological studies of curcumin
419 loaded dextran sulphate–chitosan nanoparticles. Carbohydrate Polymers.84, 3, 1158–
420 1164.

421

422 Araújo I. M. S., Zampa M. F, Moura J. B., dos Santos, Jr. J. R., Eaton P., Zucolotto V.,
423 Veras L. M. C., R de Paula. C. M., Feitosa J. P. A., Leite J. R. S. A., Eiras C., (2012).
424 Contribution of the cashew gum (*Anacardium occidentale* L.) for development of layer-
425 by-layer films with potential application in nanobiomedical devices. , Materials Science
426 & Engineering C-Materials for Biological Applications. 32, 6, 1588-1593

427

428 Ayadi F., Bayer I. S., Marras S., Athanassiou A. (2016). Synthesis of water
429 dispersed nanoparticles from different polysaccharides and their application in drug
430 release. Carbohydrate Polymer, 20, 136, 282-91.

431

432 Beck, E.W., Schneider, H., Dietzel, K., Nuernberg, B., Brune, K. (1990).
433 Gastrointestinal ulceration induced by anti-inflammatory drugs in rats. Arch
434 Toxicology, 64, 210-7.

435

436 Campos D. A., Ribeiro A. C., Costa E. M., Fernandes J. C., Tavarina F. K., Araruna F.
437 B., Eiras C., Eaton P., Leite J. R. S.A., Pintado M. M., (2012). Study of antimicrobial
438 activity and atomic force microscopy imaging of the action mechanism of cashew tree
439 gum. Carbohydrate Polymers. 90, 270– 274.

440 Chin S. F., Yazid S.N.A.M., Pang S.C. (2014) Preparation and Characterization of
441 Starch Nanoparticles for Controlled Release of Curcumin. International Journal of
442 Polymer Science, 2014.

443 Chourasia M. K., Jain S. K., (2004). Design and development of multiparticulate system
444 for targeted drug delivery to colon. Drug deliv. 11,3, 201–207.

445

446 Chourasia M. K., Jain S. K., Jain A., Soni V., Gupta Y., Jain S. K., (2006). Cross-linked
447 guar gum microspheres: a viable approach for improved delivery of anticancer drugs for
448 the treatment of colorectal cancer., AAPS PharmSciTech. 7,3, E1–E9.

449

450 David K.I., Jaidev L.R., Sethuraman S., Krishnan U. M. (2015). Dual drug loaded
451 chitosan nanoparticles—sugar-coated arsenal against pancreatic cancer. Colloids and
452 Surfaces B: Biointerfaces, 135, 689–698.

453

454

455 de Paula R. C. M., Heatley F., Budd P. M., (1998). Characterization of *Anacardium*
456 *occidentale* exudate polysaccharide. Polymer International. 45, 27–35.

457

458 de Paula, R. C. M. & Rodrigues, J. F. ,1995. Composition and rheological properties of
459 cashew tree gum, the exudate polysaccharide from *Anacardium occidentale* L.
460 Carbohydrate Polymers. 26, 3, 177–181.

461

462

- 463 Florêncio A.P.S., Melo J.H.L., Mota C.R.F.C., Melo-Júnior M.R., Araújo R.V.S.,
464 (2007). Estudo da atividade anti-tumoral do polissacarídeo (PJU) extraído de
465 *Anacardium occidentale* frente a um modelo experimental do sarcoma 180. , Revista
466 Eletrônica de. Farmácia. 4, 1, 61-65.
- 467
- 468 Galer B. S., Rowbotham M., Perander J., Devers A., Friedman E., (2000). Topical
469 diclofenac patch relieves minor sports injury pain: Results of multicenter controlled
470 clinical trial., Journal of. Pain symptom manage.19, 4, 287-294.
- 471
- 472 Gowthamarajan K., Jawahar N., Wake P., Jain K., Sood S., (2012). Development of
473 buccal tablets for curcumin using *Anacardium occidentale* gum., Carbohydrate
474 Polymers. 88, 1177– 1183.
- 475
- 476 Gowthamarajan K., Kumar G.K.P., Gaikwad N.B., Suresh B., (2011). Preliminary study
477 of *Anacardium occidentale* gum as binder in the formulation of paracetamol tablets.,
478 Carbohydrate Polymers. 83, 506–511.
- 479
- 480 Hornig S., Bunjes H., Heinze T., (2009). Preparation and characterization of
481 nanoparticles based on dextran–drug conjugates., Journal of Colloids and interface
482 science. 338, 56–62.
- 483
- 484 Jones R., Rubin G., Berenbaum F., Scheiman J., (2008). Gastrointestinal and
485 cardiovascular risks of nonsteroidal anti-inflammatory drugs., The American Journal of
486 Medicine. 121, 6, 464–474.
- 487
- 488 Kim, S., Kim, H., Jeon, O., Kwon, I. C., Park, K., (2009). Engineered polymers for
489 advanced drug delivery., European. Journal of . Pharmaceutics Biopharmaceutics. 71,
490 420-430.
- 491
- 492 Kumar R., Patil M. B., Patil S. R., Paschapur M. S., (2009).Evaluation of *Anacardium*
493 *occidentale* gum as gelling agent in aceclofenac gel., International Journal of
494 PharmTech Research. 1, 3, 695–704.
- 495

- 496 Kumari A., Yadav S. K., Yadav S. C., (2010). Biodegradable polymeric nanoparticles
497 based drug delivery systems., *Colloids and surface. B.* 75, 1, 1-18.
498
- 499 Langer R., Tirrell D.A., (2004). Designing materials for biology and medicine., *Nature.*
500 428, 487-492.
- 501 Lemarchand C., Gref R., Couvreur P., (2004). Polysaccharide-decorated nanoparticles.,
502 *Eur. J. Pharm. Biopharm.* 58, 327–341.
503
- 504 Leonard, Rouzes C., Durand A., Dellacherie E., (2003). Influence of polymeric
505 surfactants on the properties of drug-loaded PLA nanospheres., *Colloids surf. B.* 32, 2,
506 125-135.
507
- 508 Liu, Z., Jiao, Y., Wang, Y., Zhou, C., Zhang, Z., (2008). Polysaccharides-based
509 nanoparticles as drug delivery systems., *Advanced Drug Delivery Reviews*14, 1650-
510 1662.
- 511 Liu H., He J. (2005). Simultaneous release of hydrophilic and hydrophobic drugs from
512 modified chitosan nanoparticles. *Materials Letters*, 161, 415–418.
513
- 514 Liu, D. F., Ge, Y. F., Tang, Y., Yuan, Y. B., Zhang, Q., Li, R., et al. (2010). Solid lipid
515 nanoparticles for transdermal delivery of diclofenac sodium: Preparation,
516 characterization and in vitro studies. *Journal of Microencapsulation*, 27(8),726–734.
517
518
- 519 Martins A.F., de Oliveira D. M., Pereira A.G.B., Rubira A. F., Muniz E. C., (2012).
520 Chitosan/TPP microparticles obtained by microemulsion method applied in controlled
521 release of heparin., *International. Journal of Biological. Macromolecule.* 51, 1127–
522 1133.
523
- 524 Minghetti, P., Cilurzo, F., Casiraghi, A., Montanari, L., Fini, A.. (2007). Ex vivo study
525 of transdermal permeation of four diclofenac salts from different vehicles. *J. Pharm. Sci.*
526 96, 814–823.
527

- 528 Mohanraj V. J., Chen Y., (2006). Nanoparticles – A Review., Tropical Journal of
529 Pharmaceutical Research. 5, 1, 561-573.
- 530
531
- 532 Nogueira D.R., Tavano L., Mitjans M., Pérez L., Infante M. R., Vinardell M. P.,
533 (2013). In vitro antitumor activity of methotrexate via pH-sensitive chitosan
534 nanoparticles., Biomaterials. 34, 11, 2758–2772
- 535
- 536 Oh J. K., Lee D., Park J. M., (2009). Biopolymer-based microgels/nanogels for drug
537 delivery applications., Progress in Polymer Science. 34, 1261–1282
- 538
- 539 Peppas L.B., (1995). Recent advances on the use of biodegradable microparticles and
540 nanoparticles in the controlled drug delivery. International. Journal of
541 Pharmaceutics. 116, 1–9
- 542
- 543 Peppas N. A., (1985). Analysis of Fickian and non-Fickian drug release from polymers.
544 Pharmaceutica Acta Helvetiae. 60, 110-111
- 545
- 546 Piao H., Kamiya N., Hirata A., Fujii T., Goto M., (2007). A Novel Solid-in-oil
547 Nanosuspension for Transdermal Delivery of Diclofenac Sodium., Pharma. Res. 25, 4,
548 896-901
- 549 Pitombeira N. A. O., Neto J.G. V. , Silva D.A., Feitosa J.P.A., Paula H.C.B., Paula
550 R.C.M., (2015). Self-assembled nanoparticles of acetylated cashew gum:
551 Characterization and evaluation as potential drug carrier Carbohydrate Polymers 6,117,
552 610-615.
- 553
- 554 Prow T. W., Grice J.E., Lin L. L., Faye R., Butler M., Becker W., Wurm E. M.T.,
555 Yoong C., Robertson T. A., Soyer H. P., Roberts M. S., (2011). Nanoparticles and
556 microparticles for skin drug delivery., Advanced. Drug Delivery. Reviews. 63, 6, 470–
557 491
- 558

- 559 Rana V., Rai P., Tiwary A. K., Singh R. S., Kennedy J.F., Knill C. J., (2011). Modified
560 gums: Approaches and applications in drug delivery., *Carbohydrate Polymers*. 83,
561 1031–1047.
- 562
- 563 Rao , J.P. & Geckeler K. E., (2011). Polymer nanoparticles: Preparation techniques and
564 size-control parameters., *Progress in Polymer Science*. 36, 887–913
- 565 Rigopoulou, E. I., Roggenbuck, D., Smyk, D. S., Liaskos, C., Mytilinaiou, M. G., Feist,
566 E., et al. (2012). Asialoglycoprotein receptor (ASGPR) as target autoantigen in liver
567 autoimmunity: lost and found. *Autoimmunity Reviews*, 12(2), 260–269.
- 568
- 569 Rodrigues, Santos-Magalhaes N. S., Coelho L. C. B. B., Couvreur P., Ponchel G., Gref
570 R., (2003). Novel core (polyester)-shell(polysaccharide) nanoparticles: protein loading
571 and surface modification with lectins., *J. Control. Release*. 92, 103- 112.
- 572
- 573 Sarikaa P.R., Nirmala R. J., Kumarb A., Rajb D. K., Kumaryb T. V., (20015). Gum
574 arabic-curcumin conjugate micelles with enhanced loading for curcumin delivery to
575 hepatocarcinoma cells. *Carbohydrate Polymers* 134, 167–174.
- 576
- 577
- 578 Shah, P. P., Desai, P. R., Patel, A. R., Singh, M. S., (2012). Skin permeating nanogel for
579 the cutaneous co-delivery of two anti-inflammatory drugs., *Biomaterials*. 33, 5, 1607-
580 1617
- 581 Shakeel F., Baboota S., Ahuja A., Javed A., Mohammed A., Shafiq S., (2007).
582 Nanoemulsions as Vehicles for Transdermal Delivery of Aceclofenac., *AAPS Pharm.*
583 *Sci. Tech*. 8, 4, 191-199.
- 584
- 585 Shi M., Shoichet M. S., (2008). Furan-functionalized co-polymers for targeted drug
586 delivery: characterization, self-assembly and drug encapsulation., *Journal of*
587 *Biomaterial. Science., Polymer. ed*. 19, 9,1143 – 1157.
- 588

- 589 Shirato, G. V., Monteiro, F. M. F., Silva, F. O., Filho, J. L. L., Leão, A. M. A. C.,
590 (2006). O polissacarídeo do *Anacardium occidentale* L. na fase inflamatória do
591 processo cicatricial de camundongos., *Ciência. rural.* 36, 149-154.
- 592
- 593 Silva D. A. , Feitosa J.P.A, de Paula H.C.B, Paula R.C.M, , (2009). Synthesis and
594 characterization of cashew gum/acrylic acid nanoparticles., *Material Science Engineer.*,
595 29, 437-441.
- 596
- 597 Silva D. A., Paula R. C. M., . Maciel J.S, Feitosa J.P.A, de Paula H.C.B, (2010).
598 Polysaccharide-based nanoparticles formation by polyelectrolyte complexation of
599 carboxymethylated cashew gum and chitosan., *Journal of Material Science.* 45, 5605.
- 600 Silva N. H.C.S., Rodrigues A. F., Almeida I. F., Costa P. C., Rosado C., Pascoal Neto
601 C., Silvestre A. J. D., Carmen S.R. (2014). Bacterial cellulose membranes as
602 transdermal delivery systems for diclofenac: In vitro dissolution and permeation
603 studieS. *Carbohydrate Polymers*, 106, 264–269
- 604
- 605
- 606 Singh R., Lillard Jr. J. W. (2009). Nanoparticle-based targeted drug delivery.,
607 *Experimental and Molecular Pathology.* 86, 215–223.
- 608 Singh B. N., Kim K. H., (2007). Characterization and relevance of physicochemical
609 interactions among components of a novel multiparticulate formulation for colonic
610 delivery., *Int. J. Pharm.* 34, 68–77.
- 611
- 612
- 613 Sintov, A. C., Botner S., (2006). Transdermal drug delivery using microemulsion and
614 aqueous systems: Influence of skin storage conditions on the in vitro permeability of
615 diclofenac from aqueous vehicle systems., *International Journal of Pharmaceutics.* 311,
616 55–62.
- 617
- 618 Soppimath K. S., Aminabhavi T. M., Kulkarni A. R., Rudzinski W. E., (2001).
619 Biodegradable polymeric nanoparticles as drug delivery devices., *Journal of Control*
620 *Release.*, 70, 1.
- 621

622 Thambi T., Deepagan V.G., Yoon H. Y., Han H. S., Kim S.H., Son S., Jo D.G., Ahn
623 C.H., Suh Y. D., Kim K., Kwon I. C., Lee D. S., Park J. H.,(2014). Hypoxia-responsive
624 polymeric nanoparticles for tumor-targeted drug delivery., *Biomaterial.* 35, 5, 1735-
625 1743.

626

627 Torquato, D. S., Ferreira, M. L., Sá, G. C., Brito, E. S., Pinto, G. A. S., Azevedo, E. H.
628 F., (2004). Evaluation of antimicrobial activity of cashew tree gum. *World Journal of*
629 *Microbiology & Biotecnology.* 20, 505-507.

630

631 Uhrich K.E., Cannizzaro S.M, Langer R.S., Shakesheff K.M., (1999). Polymeric
632 systems for controlled drug release., *Chemical. Review.* 99, 3181–3198.

633

634 Zhang H.Z., Gao F. P., Liu L. R, Li X. M., Zhou Z. M., Yang X.D., Zhang Q. Q.,
635 (2009). Pullulan acetate nanoparticles prepared by solvent diffusion method for
636 epirubicin chemotherapy., *Colloids and surface. B.* 71, 19–26.

637

638

639

640

641

642

643

644

645

646

647

648

649

650

651

652

Table 1: Characterization of Acetylated Cashew Gum Nanoparticles

Method	Size (nm)	ζ (mV) ^a	PDI ^b	Yield (%)
Nanoprecipitation	79.37±0.608	-20.2±1.52	0.354±0.033	24
Dialysis	302.0 ±0.971	- 35.9 ± 2.49	0.187 ± 0.025	80

653

a: zeta potential

654

b: polydispersity index

655

656

657

658

659

660

Table 2: Influence of the incorporation of the drug in nanoparticles

Method	Nanoprecipitation			Dialysis		
	10:1	10:2	10:5	10:1	10:2	10:5
ACG:DDA ^a						
Size ^b	90.2±1.125**	125.9±0.776**	96.48±0.752**	262.9±4.963**	304.7±5.139	291.9±6.799
ζ (mV) ^c	-18.7±1.960	-18.8±1.410	-23.7±1.040	-31.5±0.693	-32.1±1.110	-32.9±0.741
PDI ^d	0.257±0.003	0.126±0.027	0.219±0.017	0.134±0.003	0.160±0.032	0.149±0.046
DL ^e (%)	6.6	12.1	1.8	5.9	8.2	6.4
EE ^f (%)	72.6	72.6	5.4	65.5	49.2	19.4

661

a: acetylated cashew gum: diclofenac diethylamine ratio

662

b: average size of nanoparticles

663

c: zeta potential

664

d: polydispersity index

665

e: drug loaded

666

f: encapsulation efficiency

667

**: p<0.001 compared to the drug-free nanoparticles

668

669

670

671

672

673

674
675
676
677
678
679

Figure captions

680

681 **Figure 1.** FTIR spectra of cashew gum and ACG (A) Schemes of the acetylated cashew
682 gum (B).
683

684 **Figure 2.** Nanoparticle size distribution of ACG-NPs and DDA-ACG-NPs (A)
685 synthesized by nanoprecipitation and (B) synthesized by dialysis. (nanoparticle:drug
686 ratio 10:1)

687 **Figure 3.** SEM images of ACG nanoparticles without (B) and with DDA (A).

688 **Figure 4.** Cell viability for OSCC where CT = control, ACG-NPs = acetylated cashew
689 gum nanoparticles, DDA-ACG-NPs = acetylated cashew gum nanoparticles loaded with
690 diclofenac diethylamine: (A) according to the polymer concentration (1 = 50 $\mu\text{g/ml}$, 2 =
691 75 $\mu\text{g/ml}$, and 3 = 100 $\mu\text{g/ml}$ and 4 = 150 $\mu\text{g/ml}$) and (B) according to the drug
692 concentration (n=3).

693

694 **Figure 5.** *In vitro* release profile for diclofenac A. DDA-ACG-NPs B free DDA (n=3)

695 **Figure 6.** Mechanism associated with *in vitro* release of diclofenac from DDA-ACG-
696 NPs, according to the Korsmeyer-Peppas model (n =3).

697 **Figure 7.** Percutaneous penetration of DDA through pig skin after application of the
698 drug as free DDA and in DDA-ACG-NPs (n=5).

699

700

701

702

703

704

705

706

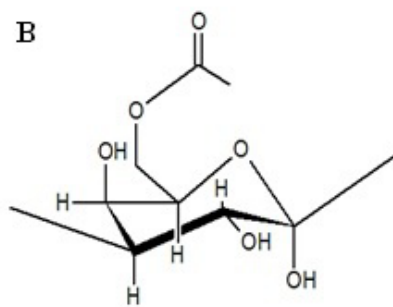
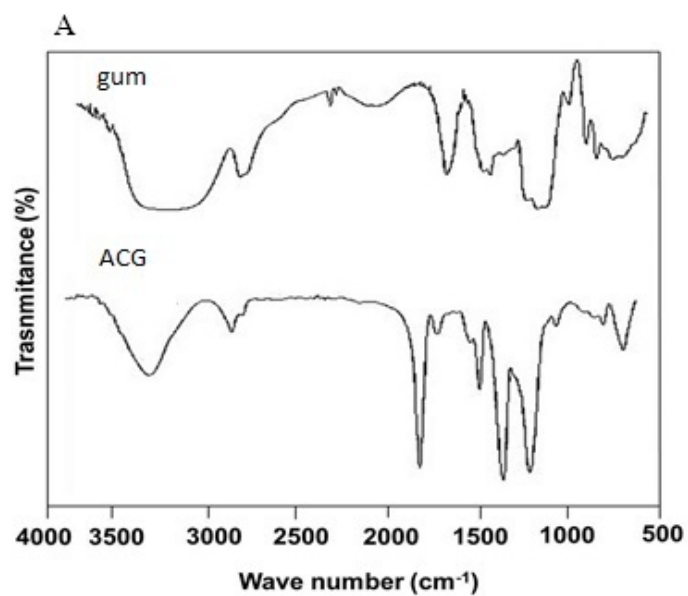
707

708

709

710

711
712
713
714
715
716
717



718
719
720
721
722
723
724
725
726
727
728
729
730
731

Figure 1

732
733
734
735
736
737
738
739
740
741
742
743
744
745
746
747
748
749
750
751
752
753
754
755
756
757
758
759
760
761
762

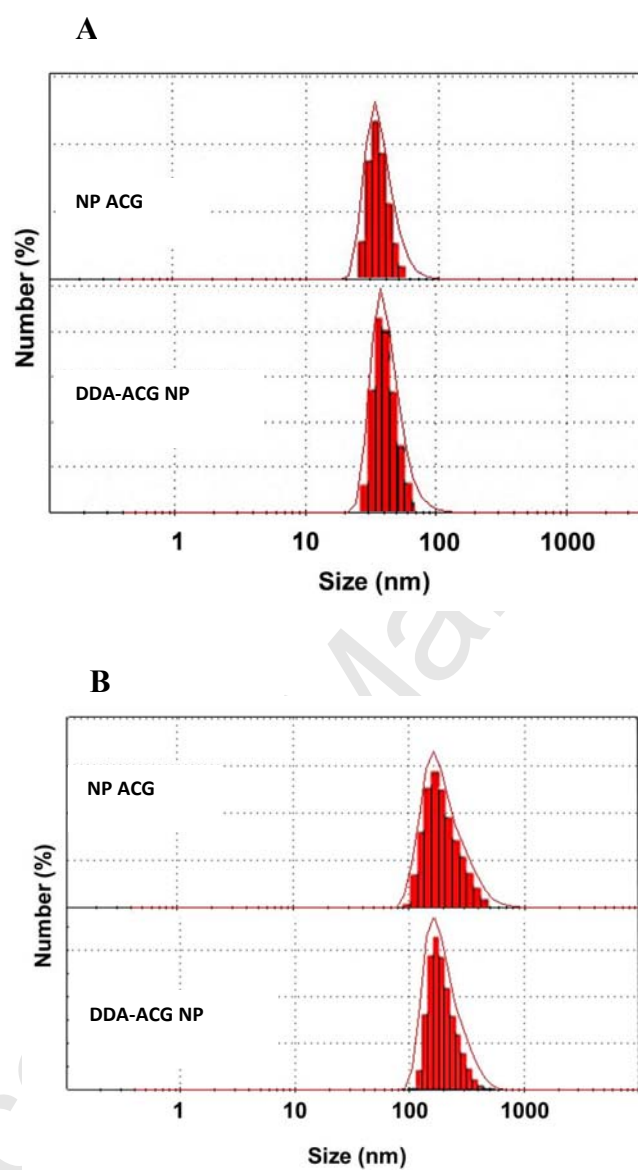


Figure 2

763

764

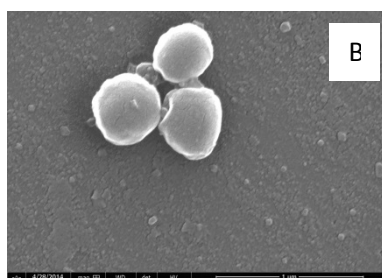
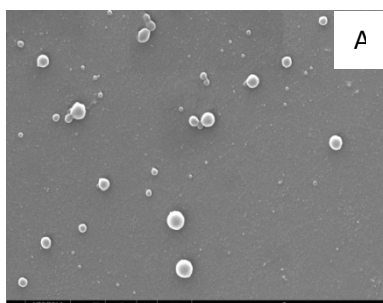
765

766

767

768

769



770

771

772

773

774

775

776

777

778

779

Figure 3.

780

781

782

783

784

785

786

787

788

789

790

791

792

793

794

795

796

797

798

799

800

801

802

803

804

805

806

807

808

809 **Figure 4.**

810

811

812

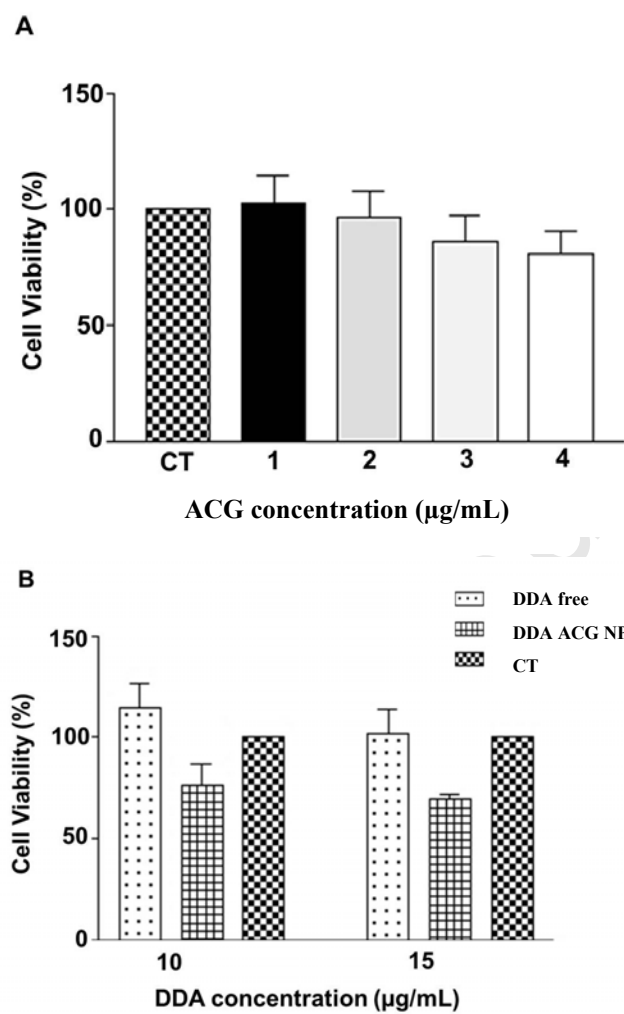
813

814

815

816

817



818

819

820

821

822

823

824

825

826

827

828

829

830

831

832

833

834

835

836 **Figure 5.**

837

838

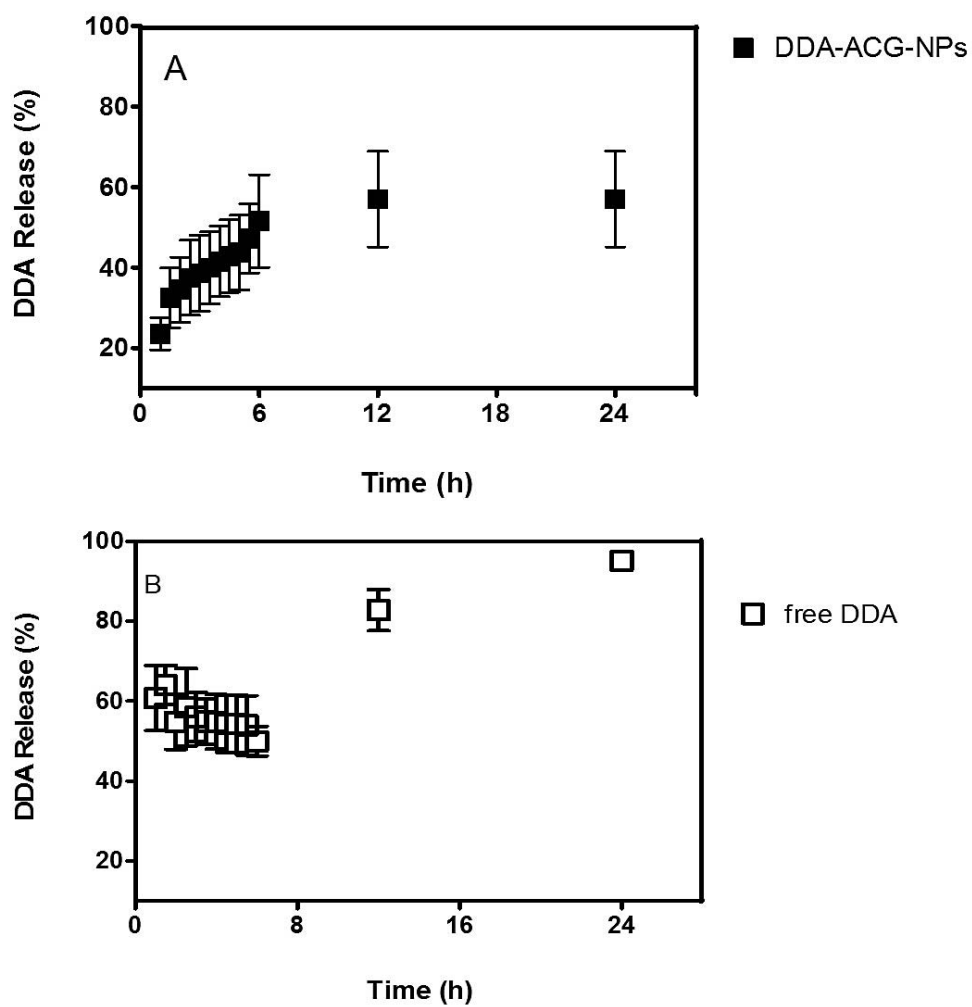
839

840

841

842

843



844

845

846

847

848

849

850

851

852

853

854

855

856

857

858

859 **Figure 6**

860

861

862

863

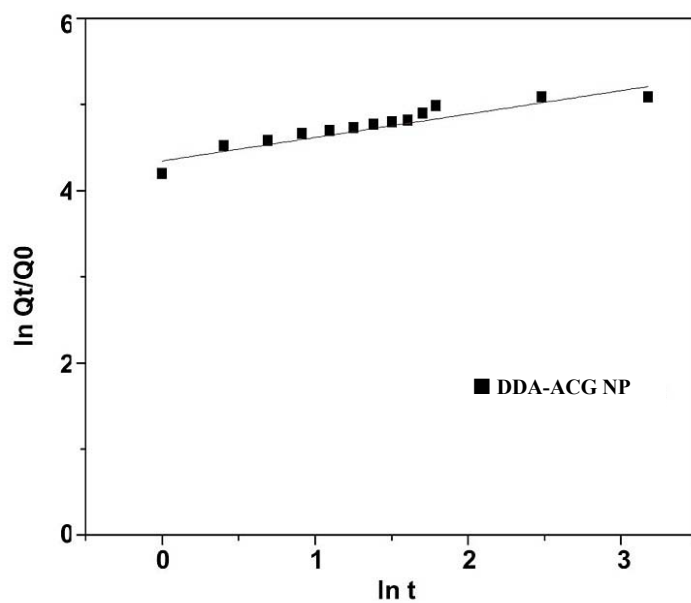
864

865

866

867

868



869

870

871

872

873

874

875

876

877

878

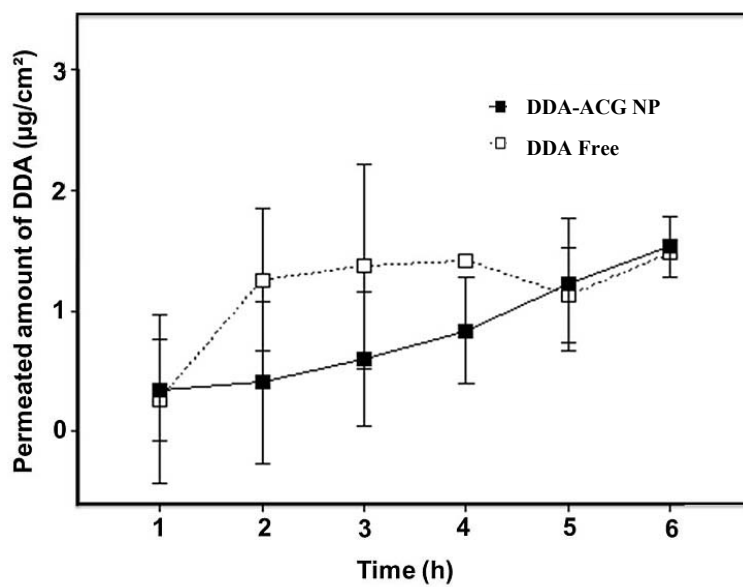
879

880

881

882

883

**Figure 7**